

A New Alluaudite-like Phosphate, $\text{Na}_{1.67}\text{Co}_{2.45}\text{Cr}_{0.78}(\text{PO}_4)_3$: Synthesis and Crystal Structure

Sirine El Arni*, Mohammed Hadouchi, Jamal Khmiyas, Abderrazzak Assani, Mohamed Saadi and Lahcen El Ammari

Laboratoire de Chimie Appliquée des Matériaux, Centre des Sciences des Matériaux, Faculty of Science, Mohammed V University in Rabat, Avenue Ibn Battouta, BP 1014, Rabat, Morocco

*Correspondence to:

Sirine El Arni
Laboratoire de Chimie Appliquée des Matériaux,
Centre des Sciences des Matériaux,
Faculty of Science,
Mohammed V University in Rabat,
Avenue Ibn Battouta,
BP 1014, Rabat, Morocco.
E-mail: sirine.elarni@um5r.ac.ma

Received: July 25, 2023

Accepted: September 27, 2023

Published: September 29, 2023

Citation: El Arni S, Hadouchi M, Khmiyas J, Assani A, Saadi M, et al. 2023. A New Alluaudite-like Phosphate, $\text{Na}_{1.67}\text{Co}_{2.45}\text{Cr}_{0.78}(\text{PO}_4)_3$: Synthesis and Crystal Structure. *NanoWorld J* 9(S2): S425-S430.

Copyright: © 2023 El Arni et al. This is an Open Access article distributed under the terms of the Creative Commons Attribution 4.0 International License (CCBY) (<http://creativecommons.org/licenses/by/4.0/>) which permits commercial use, including reproduction, adaptation, and distribution of the article provided the original author and source are credited.

Published by United Scientific Group

Abstract

The development of new phosphate materials has attracted huge attention because of their promising applications as electrode materials and solid-state electrolytes for next-generation batteries. Several phosphates were elaborated and structurally investigated, such as the NASICON and alluaudite families, which show promising structural features permitting electrochemical activity as electrodes for rechargeable Li/Na batteries. In the context of the elaboration and structural investigation of novel alluaudite phosphates, we report on the crystal growth and the structural investigation of a new sodium, cobalt, and chromium-based phosphate, $\text{Na}_{1.67}\text{Co}_{2.45}\text{Cr}_{0.78}(\text{PO}_4)_3$, with an alluaudite-type structure. This phosphate has been produced using a solid-state technique and its structure has been elucidated thanks to single-crystal X-ray diffraction (XRD) data. The title compound crystallizes in space group C2/c of the monoclinic system with the lattice parameters $a = 11.7538(3) \text{ \AA}$, $b = 12.3671(3) \text{ \AA}$, $c = 6.4180(2) \text{ \AA}$, and $\beta = 114.022(10)^\circ$. Its structure is formed by infinite chains, which are in turn created from edge-sharing $(\text{Co}_1, \text{Cr}_1)_2\text{O}_{10}$ units and Co_2O_6 octahedra. These infinite chains are bonded together by the PO_4 tetrahedra, resulting in a three-dimensional framework with two different kinds of hexagonal tunnels where Na^+ and $\text{Na}^+/\text{Co}^{2+}$ cations can be found.

Keywords

Phosphate, Crystal structure, Solid-state reaction, Alluaudite family, Single crystal X-ray diffraction

Introduction

The development of transition metal-based materials with structures exhibiting tunnels or layers has gained prominence because of their prospective uses in a variety of domains, including catalytic activity [1] and electrochemistry as electrode materials for Li-ion and Na-ion batteries [2-4]. In recent years, transition metal-based materials belonging to the phosphate class have been highly investigated due to their rich structural chemistry. Several phosphates, including the NASICON and alluaudite families, have been developed and structurally investigated, with promising structural features allowing electrochemical activity as electrodes for rechargeable Li/Na batteries.

As it is well known, Fisher [5] was the first to identify the crystal structure of the natural alluaudite, demonstrating that this type of compound crystallizes in monoclinic symmetry with the space group C2/c. Subsequently, Moore has established a general structural formula for materials belonging to the alluaudite family, $\text{X}(2)\text{X}(1)\text{M}(1)\text{M}(2)_2(\text{PO}_4)_3$, where X and M cations are listed in decreasing order of size; accordingly, monovalent and divalent cations can reside in the

X sites, while the octahedral M site can accommodate both bivalent and trivalent cations [6]. More recently, Hatert has demonstrated based on detailed structural studies, the presence of three cationic sites in channels with crystallographic locations distinct from those of X(1) and X(2) and presented a new generic formula [A(2)A(2)']₂[A(1)A(1)']₂M(1)M(2)₂(PO₄)₃ for alluaudite-type materials [7]. The literature survey shows the rich structural chemistry of the alluaudite family, which can accommodate a variety of transition metals. Moreover, further study has broadened the alluaudite-type structure into a variety of vanadates, arsenates, sulfates, molybdates, and tungstates [8-14]. Thus, making alluaudites with a range of anionic groups and a broad variety of transition metals can also produce more desirable features such as magnetism [15-17] and electronic and/or ionic conductivity [18-20], whereas Fe-based alluaudites demonstrate an excellent thermal stability [21-23]. Additionally, alluaudite-type materials have garnered considerable interest for sodium and lithium batteries due to their intriguing open framework and alkali site vacancies that promote efficient Li/Na ion migration, which is appropriate for battery applications. For example, Na₂Fe₂(SO₄)₃, which only includes divalent Fe ions, was tested as a cathode for Na-ion batteries. This compound has been considered the first alluaudite cathode to exhibit the highest voltage and highest energy density of any alluaudite cathode previously discovered [24].

Indeed, one of our primary goals is to synthesize and characterize new transition metal-based materials from the well-known alluaudite family, as well as to investigate their structure-property relationship. In this framework, we have reported new alluaudite-like phosphates and vanadates such as Na₂Co₂Cr(PO₄)₃ [25], A₂Co₂FeVO₄ (A = Na and Ag) [16, 26] and Na₂Zn₂Fe(VO₄)₃ [15].

In the context of the elaboration and structural study of novel phosphates, this paper details the findings of our investigation on the crystal growth and the structural investigation of a non-stoichiometric phosphate containing sodium, cobalt, and chromium as a novel element of the alluaudite family, precisely Na_{1.67}Co_{2.45}Cr_{0.78}(PO₄)₃.

Materials and Method

Single crystals synthesis

The Na_{1.67}Co_{2.45}Cr_{0.78}(PO₄)₃ phosphate was produced using a solid-state reaction from a starting mixture of NaNO₃ (≥ 99%, Merck), (CH₃COO)₂Co·4H₂O (≥ 99%, Merck), Cr(NO₃)₃·9H₂O (≥ 98%, Merck), and NH₄H₂PO₄ (≥ 99.6%, Acros Organics), which were weighted and mixed in the appropriate amounts corresponding to the molar ratios Na:Co:Cr:P = 2:2:1:3. The mixture was placed in a platinum crucible and gradually heated until it reached the melting point of 1343 K. At a cooling rate of 5 K/h to room temperature, the molten product solidified into dark brown crystals with sufficient size for XRD analysis.

Structure determination

For the purpose of collecting XRD data, a suitable single crystal was chosen under a microscope. The title compound's

XRD data were obtained using a Bruker D8 Venture Super DUO diffractometer with a PHOTON100 CMOS area-detector and monochromatic MoK α radiation ($\lambda = 0.71073$ Å) at room temperature (296 K). Data were gathered using APEX3 [27] software, and SADABS [28] was utilized to develop a multi-scan semi-empirical technique for the absorption correction. The direct method was used to solve the crystal structure, and SHELXT 2013 [29] and SHELXL 2013 [30], both of which were included in the WinGX software package [31] were used to refine it. The structure is determined at nanometric scale.

Results and Discussion

Using single crystal XRD data, the structure of the title chemical was determined in the monoclinic C2/c symmetry. The parameters of the measured unit cell are: $a = 11.7538(3)$ Å, $b = 12.3671(3)$ Å, $c = 6.4180(2)$ Å, $\beta = 114.0220(10)^\circ$, and $V = 852.12(4)$ Å³. A summary of the crystal data, the data collection, as well as the structure refinement parameters of the phosphate Na_{1.67}Co_{2.45}Cr_{0.78}(PO₄)₃ are depicted in table 1. Fractional atomic coordinates, anisotropic displacement parameters of all atoms and selected geometric parameters are listed in table 2, table 3, and table 4, respectively.

In the structure of this orthophosphate, the phosphorus atoms are positioned in the 8*f* and 4*e* Wyckoff positions of the C2/c space group. Additionally, cobalt and chromium share the 8*f* general position with Co²⁺/Cr³⁺ occupancy fractions of 0.607/0.393, while the second cobalt fully occupies the 4*e* position. The sodium cations take up the 4*e* and 4*b* special po-

Table 1: Crystallographic data, data collection, and refinement structure details of Na_{1.67}Co_{2.45}Cr_{0.78}(PO₄)₃.

Crystal data	
Chemical formula	Na _{1.67} Co _{2.45} Cr _{0.78} (PO ₄) ₃
M_r (g/mol)	510.63
Crystal system, space group	Monoclinic, C2/c
a, b, c (Å)	11.7538 (3), 12.3671 (3), 6.4180 (2)
β (°)	114.022 (1)
V (Å ³)	852.12 (4)
Z	4
μ (mm ⁻¹)	6.42
Data collection	
Diffractometer	Bruker D8 Venture
Absorption correction	Multi-scan (SADABS [28])
No. of measured, independent and observed [$I > 2\sigma(I)$] reflections	18619, 2260, 2164
R_{int}	0.031
$\theta_{min} - \theta_{max}$ (°)	2.5 - 37.6
$(\sin\theta/\lambda)_{max}$ (Å ⁻¹)	0.858
Temperature (K)	296
Radiation type	X-ray, Mo K α radiation ($\lambda=0.71073$ Å)
Refinement	
$R[F^2 > 2s(F^2)], \omega R(F^2), S$	0.018, 0.047, 1.06
No. of reflections	2260
No. of parameters	97
$\Delta\rho_{max}, \Delta\rho_{min}$ (e Å ⁻³)	0.74, -1.01

Table 2: Atomic coordinates and equivalent isotropic displacement parameters (\AA^2) for $\text{Na}_{1.67}\text{Co}_{2.45}\text{Cr}_{0.78}(\text{PO}_4)_3$.

	Wyck.	x	y	z	U_{eq}	Occ.
Cr1	8f	0.21831 (2)	0.15946 (2)	0.13219 (2)	0.00556 (4)	0.393 (8)
Co1	8f	0.21831 (2)	0.15946 (2)	0.13219 (2)	0.00556 (4)	0.607 (8)
Co2	4e	0.0000	0.26776 (2)	0.2500	0.00775 (5)	0.500
Co3	4b	0.0000	0.5000	0.0000	0.0299 (3)	0.238 (3)
Na1	4b	0.0000	0.5000	0.0000	0.0299 (3)	0.762 (3)
Na2	4e	0.5000	0.51481 (11)	0.7500	0.0342 (3)	1
P1	8f	0.26381 (2)	0.39099 (2)	0.37357 (4)	0.00546 (5)	1
P2	4e	0.0000	0.29076 (3)	-0.2500	0.00512 (6)	1
O1	8f	0.27651 (8)	0.32173 (7)	0.18298 (13)	0.00968 (13)	1
O2	8f	0.33601 (8)	0.33378 (6)	0.60554 (14)	0.00985 (13)	1
O3	8f	0.32682 (8)	0.50060 (7)	0.38553 (15)	0.01120 (14)	1
O4	8f	0.12520 (8)	0.40026 (7)	0.32293 (17)	0.01271 (15)	1
O5	8f	0.04073 (7)	0.21828 (7)	-0.03443(13)	0.00821 (12)	1
O6	8f	0.10148 (8)	0.36784 (7)	-0.25160 (16)	0.01291 (15)	1

Table 3: Anisotropic displacement parameters (\AA^2) of all atoms.

	U^{11}	U^{22}	U^{33}	U^{12}	U^{13}	U^{23}
Cr1	0.00506 (6)	0.00640 (6)	0.00543 (6)	-0.00033 (4)	0.00235 (5)	-0.00023 (4)
Co1	0.00506 (6)	0.00640 (6)	0.00543 (6)	-0.00033(4)	0.00235 (5)	-0.00023 (4)
Co2	0.00781 (9)	0.00799 (9)	0.00895 (9)	0.000	0.00496 (6)	0.000
Co3	0.0446 (5)	0.0085 (3)	0.0143 (3)	0.0003 (2)	-0.0107 (2)	-0.00122 (18)
Na1	0.0446 (5)	0.0085 (3)	0.0143 (3)	0.0003 (2)	-0.0107 (2)	-0.00122 (18)
Na2	0.0193 (4)	0.0526 (7)	0.0247 (5)	0.000	0.0026 (4)	0.000
P1	0.00599 (10)	0.00518 (10)	0.00500(10)	-0.00019 (7)	0.00201 (8)	0.00032 (7)
P2	0.00459 (13)	0.00549 (13)	0.00466(13)	0.000	0.00126 (10)	0.000
O1	0.0113 (3)	0.0120 (3)	0.0061 (3)	0.0005 (2)	0.0039 (2)	-0.0012 (2)
O2	0.0147 (3)	0.0083 (3)	0.0058 (3)	0.0022 (2)	0.0034 (3)	0.0017 (2)
O3	0.0115 (3)	0.0083 (3)	0.0130 (3)	-0.0026 (2)	0.0042 (3)	0.0027 (3)
O4	0.0075 (3)	0.0095 (3)	0.0217 (4)	-0.0001 (2)	0.0065 (3)	-0.0010 (3)
O5	0.0066 (3)	0.0121 (3)	0.0053 (3)	0.0004 (2)	0.0018 (2)	0.0020 (2)
O6	0.0090 (3)	0.0108 (3)	0.0174 (4)	-0.0032 (3)	0.0039 (3)	0.0029 (3)

sitions; the 4b site is occupied with 76% of Na^+ and 24% of Co^{2+} , while the 4e site is fully occupied by Na2. The oxygen is all located at 8f Wyckoff position. The obtained low values of the reliability factors ensure the effectiveness of this structural model, with $R = 1.8\%$, $wR = 4.7\%$, and $S = 1.06$ (See table 1).

The environment of each atom is presented in figure 1a. The $\text{Co}^{2+}/\text{Cr}^{3+}-\text{O}$ distances range from 1.9662 (9) \AA to 2.1024 (9) \AA , which highlights a moderate distortion of the $(\text{Co1}/\text{Cr1})\text{O}_6$ octahedron as a result of the cationic disorder. Likewise, the Co2O_6 octahedron is highly deformed, as shown in figure 1a and the $\text{Co2}-\text{O}$ distances vary between 2.1234 (9) \AA and 2.1672(8) \AA . The phosphorus atoms are arranged in tetrahedral environments. This compound's crystal structure is made up of infinite chains that run along the [101] direction of two edge-sharing $[\text{Co1}/\text{Cr1O}_6]$ octahedra, resulting in the formation of $[(\text{Co1},\text{Cr1})_2\text{O}_{10}]$ dimers that are associated by a joint edge to the highly distorted Co2O_6 octahedra as shown in figure 1c. These chains are connected via the corners shared

by P1O_4 and P2O_4 tetrahedra, building layers perpendicular to the [010] direction (Figure 1c). The structure can therefore be visualized as parallel sheets which are joined along the c axis by PO_4 units. These layers form a three-dimensional architecture including two large c -directional channels with distinct hexagonal shapes in which the Na1 and Na2/Co3 cations are located (Figure 1e). The mixed site (Na1/Co3) and the Na2 site are both surrounded by eight oxygen atoms (Figure 1a). The Na/Co—O distances are in the range of 2.2555(9)–2.8757(10) \AA , while the Na2—O bond length varies between 2.4019(9) and 2.8517(14) \AA . It's worth noting that there are several other examples of compounds with cationic disorder and structures similar to the title phosphate, such as $\text{Na}_{1.25}\text{Mg}_{1.10}\text{Fe}_{1.90}(\text{PO}_4)_3$ and $\text{Na}_{1.67}\text{Zn}_{1.67}\text{Fe}_{1.33}(\text{PO}_4)_3$ in which eight oxygen atoms enclose the sodium cations [32, 33].

As it is well known, the alluaudite compounds hold significant promise as electrode materials and solid-state electrolytes for next-generation batteries. Their appealing charac-

Table 4: Main interatomic distances (Å) and angles (°) in $\text{Na}_{1.67}\text{Co}_{2.45}\text{Cr}_{0.78}(\text{PO}_4)_3$.

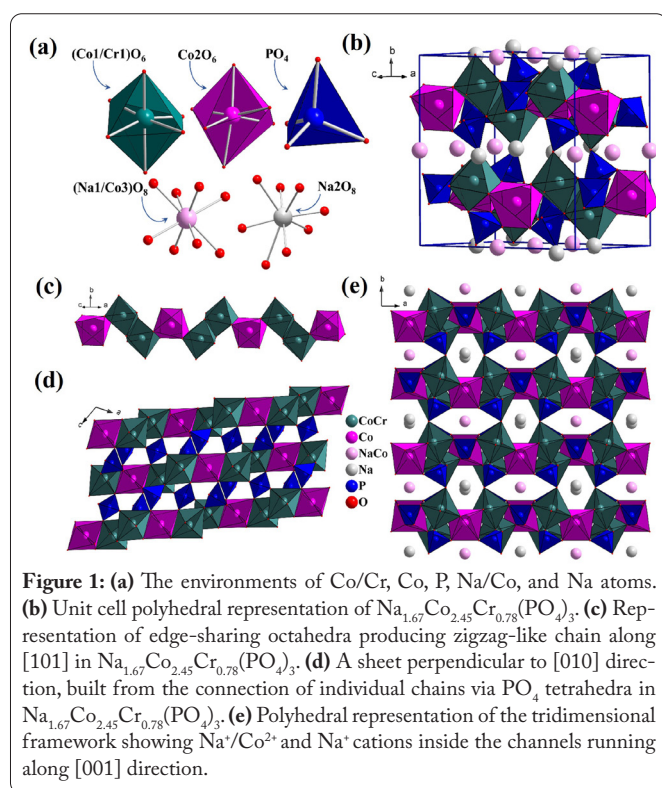
Atom	Distances (Å) Co1/Cr1—O			
Co1/Cr1	Co1/Cr1—O6 ⁱ	1.9662 (9)	Co1/Cr1—O5	2.0523 (8)
	Co1/Cr1—O3 ⁱⁱ	2.0261 (9)	Co1/Cr1—O1 ⁱ	2.0615 (8)
	Co1/Cr1—O2 ⁱⁱⁱ	2.0305 (9)	Co1/Cr1—O1	2.1024 (9)
Co1/Cr1	Angles (°) O—Co1/Cr1—O			
	O6 ⁱ —Co1/Cr1—O3 ⁱⁱ	94.09(4)	O3 ⁱⁱ —Co1/Cr1—O1 ⁱ	99.56 (4)
	O6 ⁱ —Co1/Cr1—O2 ⁱⁱⁱ	109.65 (4)	O2 ⁱⁱⁱ —Co1/Cr1—O1 ⁱ	162.49 (3)
	O3 ⁱⁱ —Co1/Cr1—O2 ⁱⁱⁱ	85.58 (3)	O5—Co1/Cr1—O1 ⁱ	83.04 (3)
	O6 ⁱ —Co1/Cr1—O5	165.85 (4)	O6 ⁱ —Co1/Cr1—O1	82.68 (4)
	O3 ⁱⁱ —Co1/Cr1—O5	97.29 (3)	O3 ⁱⁱ —Co1/Cr1—O1	174.58 (3)
	O2 ⁱⁱⁱ —Co1/Cr1—O5	79.69 (3)	O2 ⁱⁱⁱ —Co1/Cr1—O1	91.40 (3)
	O6 ⁱ —Co1/Cr1—O1 ⁱ	86.81 (4)	O5—Co1/Cr1—O1	86.57 (3)
O1 ⁱ —Co1/Cr1—O1	84.65 (3)			
Co2	Distances (Å) Co2—O			
	Co2—O4 ^v	2.1234 (9)	Co2—O5	2.1558 (8)
	Co2—O4	2.1234 (9)	Co2—O2 ^{vi}	2.1672 (8)
Co2—O5 ^v	2.1557 (8)	Co2—O2 ⁱⁱⁱ	2.1672 (8)	
Co2	Angles (°) O—Co2—O			
	O4 ^v —Co2—O4	78.99 (5)	O4—Co2—O2 ^{vi}	163.20 (3)
	O4 ^v —Co2—O5 ^v	91.88 (3)	O5 ^v —Co2—O2 ^{vi}	74.48 (3)
	O4—Co2—O5 ^v	113.91 (3)	O5—Co2—O2 ^{vi}	86.49 (3)
	O4 ^v —Co2—O5	113.91 (3)	O4 ^v —Co2—O2 ⁱⁱⁱ	163.20 (3)
	O4—Co2—O5	91.88 (3)	O4—Co2—O2 ⁱⁱⁱ	86.39 (3)
	O5 ^v —Co2—O5	147.02 (5)	O5 ^v —Co2—O2 ⁱⁱⁱ	86.49 (3)
	O4 ^v —Co2—O2 ^{vi}	86.39 (3)	O5—Co2—O2 ⁱⁱⁱ	74.48 (3)
O2 ^{vi} —Co2—O2 ⁱⁱⁱ	109.18 (5)			
P1	Distances (Å) P1—O			
	P1—O4	1.5303 (9)	P1—O1	1.5495 (8)
P1—O3	1.5315 (9)	P1—O2	1.5520 (8)	
P1	Angles (°) O—P1—O			
	O4—P1—O3	113.31 (5)	O4—P1—O2	110.92 (5)
	O4—P1—O1	108.06 (5)	O3—P1—O2	106.92 (5)
O3—P1—O1	109.19 (5)	O1—P1—O2	108.33 (5)	
P2	Distances (Å) P2—O			
	P2—O6	1.5303 (9)	P2—O5	1.5516 (8)
P2—O6 ^{viii}	1.5303 (9)	P2—O5 ^{viii}	1.5516 (8)	
P2	Angles (°) O—P2—O			
	O6—P2—O6 ^{viii}	102.93 (7)	O6—P2—O5 ^{viii}	108.20 (5)
	O6—P2—O5	114.05 (4)	O6 ^{viii} —P2—O5 ^{viii}	114.05 (4)
O6 ^{viii} —P2—O5	108.19 (5)	O5—P2—O5 ^{viii}	109.43 (7)	
Na1/Co3	Distances (Å) Na1/Co3—O			
	Na1/Co3—O6 ^{vi}	2.2555 (9)	Na1/Co3—O4 ^{ix}	2.5180 (9)
	Na1/Co3—O6 ^{vii}	2.2555 (9)	Na1/Co3—O4 ^{iv}	2.5180 (9)
	Na1/Co3—O4	2.3450 (9)	Na1/Co3—O6	2.8757 (10)
Na1/Co3—O4 ^{viii}	2.3450 (9)	Na1/Co3—O6 ^{viii}	2.8758 (10)	
Na2	Distances (Å) Na2—O			
	Na2—O3 ^x	2.4019 (9)	Na2—O5 ^{xii}	2.8172 (15)
	Na2—O3	2.4019 (9)	Na2—O5 ^{xiii}	2.8172 (15)
	Na2—O3 ^{vii}	2.5253 (9)	Na2—O2	2.8517 (14)
Na2—O3 ^{xi}	2.5253 (9)	Na2—O2 ^x	2.8517 (14)	

Note: Symmetry codes: (i) $-x+1/2, -y+1/2, -z$; (ii) $-x+1/2, y-1/2, -z+1/2$; (iii) $-x+1/2, -y+1/2, -z+1$; (iv) $-x, y, -z+1/2$; (v) $x-1/2, -y+1/2, z-1/2$; (vi) $x, -y+1, z+1/2$; (vii) $-x, y, -z-1/2$; (viii) $-x, -y+1, -z$; (ix) $x, -y+1, z-1/2$; (x) $-x+1, y, -z+3/2$; (xi) $-x+1, -y+1, -z+1$; (xii) $x+1/2, y+1/2, z+1$; (xiii) $-x+1/2, y+1/2, -z+1/2$.

teristics, such as high theoretical capacity, favorable insertion/extraction properties and stability make them attractive candidates for Na-ion and Li-ion batteries. Moreover, their potential applications extend beyond batteries, making them versatile

materials for various energy storage and conversion devices. Ongoing research and development efforts aim to further optimize alluaudite compounds for enhanced performance and commercial viability in the energy storage sector. Therefore, it

is intriguing to explore the phosphate $\text{Na}_{1.67}\text{Co}_{2.45}\text{Cr}_{0.78}(\text{PO}_4)_3$ in this area, which will be the subject of the future work. Nothing that the specific arrangement of Na, Co and Cr ions in the alluaudite-type structure plays a crucial role in determining its potential electrochemical activity. This arrangement influences several key aspects that affect the compound's performance as an electrode material or solid-state electrolyte for next-generation batteries. For example, the arrangement of Na ions within the tunnels of the alluaudite structure is favorable for their mobility and accessibility for electrochemical reactions. Na ions must be able to easily navigate the material's lattice during charge and discharge cycles. Additionally, both Co and Cr ions may participate and offer high redox potential during battery operation. The arrangement of these ions influences their ability to undergo oxidation and reduction processes, which are crucial for storing and releasing electrical energy.



Conclusion

Single crystals of a new orthophosphate $\text{Na}_{1.67}\text{Co}_{2.45}\text{Cr}_{0.78}(\text{PO}_4)_3$ were successfully produced by a solid-state reaction route. Its structure is determined from single-crystal XRD data. This phosphate crystallizes with the alluaudite-type structure. Its three-dimensional structure is composed of edge-sharing $(\text{Co1}/\text{Cr1})\text{O}_6$ octahedra that form $(\text{Co1}/\text{Cr1})\text{O}_{11}$ dimers. These dimers are linked together by Co_2O_6 octahedra to construct infinite $-(\text{Co1}/\text{Cr1})_2-\text{Co}_2-$ chains that run along the [101] axis. The joining of these chains via PO_4 tetrahedra results in a three-dimensional structure defining two large channels with distinct hexagonal shapes running along the c-direction and containing the Na_2 and $\text{Na1}/\text{Co3}$ cations.

Acknowledgements

The X-ray measurements were performed at Faculty of Science Mohammed V University in Rabat, which the authors gratefully acknowledge.

Conflict of Interest

The authors affirm that there are no competing financial interests or personal relationships that could influence the findings reported in this paper.

Funding

The CNRST (Centre National pour la Recherche Scientifique et Technique) funded this research through the Excellence Research Scholarships Program.

References

- Cheetham AK, Férey G, Loiseau T. 1999. Open-framework inorganic materials. *Angew Chemie Int Ed* 38(22): 3268-3292. [https://doi.org/10.1002/\(SICI\)1521-3773\(19991115\)38:22<3268::AID-ANIE3268>3.0.CO;2-U](https://doi.org/10.1002/(SICI)1521-3773(19991115)38:22<3268::AID-ANIE3268>3.0.CO;2-U)
- Natarajan S, Mandal S. 2008. Open-framework structures of transition-metal compounds. *Angew Chemie Int Ed* 47(26): 4798-4828. <https://doi.org/10.1002/anie.200701404>
- Hadouchi M, Koketsu T, Hu Z, Ma J. 2022. The origin of fast-charging lithium iron phosphate for batteries. *Battery Energy* 1(1): 20210010. <https://doi.org/10.1002/bte2.20210010>
- Ellis BL, Makahnouk WRM, Makimura Y, Toghill K, Nazar LF. 2007. A multifunctional 3.5 V iron-based phosphate cathode for rechargeable batteries. *Nat Mater* 6(10): 749-753. <https://doi.org/10.1038/nmat2007>
- Fisher DJ. 1955. Alluaudite. *Am Miner* 40(11-12): 1100-1109.
- Moore PB. 1971. Crystal chemistry of the alluaudite structure type: contribution to the paragenesis of pegmatite phosphate giant crystals. *Am Miner* 56(11-12): 1955-1975.
- Hatert F. 2019. A new nomenclature scheme for the alluaudite supergroup. *Eur J Miner* 31(4): 807-822. <https://doi.org/10.1127/ejm/2019/0031-2874>
- Yahia HB, Shikano M, Essehli R, Belharouak I. 2016. Crystal structure of the alluaudite $\text{Ag}_3\text{Mn}_3(\text{VO}_4)_3$. *Zeitschrift Für Kristallstruktur* 231(5): 267-270. <https://doi.org/10.1515/zkri-2016-1930>
- Khorari S, Rulmont A, Tarte P. 1997. Alluaudite-like structure of the arsenate $\text{Na}_3\text{In}_2(\text{AsO}_4)_3$. *J Solid State Chem* 134(1): 31-37. <https://doi.org/10.1006/jssc.1997.7526>
- Đorđević T, Wittwer A, Krivovichev SV. 2015. Three new alluaudite-like protonated arsenates: $\text{NaMg}_3(\text{AsO}_4)(\text{AsO}_3\text{OH})_2$, $\text{NaZn}_3(\text{AsO}_4)(\text{AsO}_3\text{OH})_2$ and $\text{Na}(\text{Na}_{0.6}\text{Zn}_{0.4})\text{Zn}_2(\text{H}_{0.6}\text{AsO}_4)(\text{AsO}_3\text{OH})_2$. *Eur J Miner* 27(4): 559-573. <https://doi.org/10.1127/ejm/2015/0027-2458>
- Tait KT, Hawthorne FC, Halden NM. 2021. Alluaudite-group phosphate and arsenate minerals. *Can Miner* 59(1): 243-263. <https://doi.org/10.3749/canmin.2000057>
- Jungers T, Mahmoud A, Malherbe C, Boschini F, Vertruyen B. 2019. Sodium iron sulfate alluaudite solid solution for Na-ion batteries: moving towards stoichiometric $\text{Na}_2\text{Fe}_2(\text{SO}_4)_3$. *J Mater Chem A* 7(14): 8226-8233. <https://doi.org/10.1039/c9ta00116f>
- Serdtshev AV, Solodovnikov SF, Medvedeva NI. 2020. Sodium diffusion and redox properties of alluaudite $\text{Na}_{2-2x}\text{M}_{2-2x}(\text{MoO}_4)_3$ (M = Fe, Co, Ni) from DFT+U study. *Mater Today Commun* 22: 100825. <https://doi.org/10.1016/j.mtcomm.2019.100825>

- Solodovnikov SF, Gulyaeva OA, Savina AA, Yudin VN, Buzlukov AL, et al. 2022. Molybdates and tungstates of the alluaudite family: crystal chemistry, composition, and ionic mobility. *J Struct Chem* 63(7): 1101-1133. <https://doi.org/10.1134/S0022476622070071>
- Lamsakhar NEH, Hadouchi M, Zriouil M, Assani A, Saadi M, et al. 2019. A novel alluaudite-type vanadate, $\text{Na}_2\text{Zn}_2\text{Fe}(\text{VO}_4)_3$: synthesis, crystal structure, characterization and magnetic properties. *Inorg Chem Commun* 107: 107472. <https://doi.org/10.1016/j.inoche.2019.107472>
- Hadouchi M, Assani A, Saadi M, Lahmar A, El Marsi M, et al. 2019. Synthesis, characterization, and magnetic properties of $\text{A}_2\text{Co}_2\text{Fe}(\text{VO}_4)_3$ (A = Ag or Na) alluaudite-type vanadates. *J Supercond Nov Magn* 32: 2437-2446. <https://doi.org/10.1007/s10948-018-4964-5>
- Benhsina E, Hermouche L, Assani A, Saadi M, Labjar N, et al. 2021. Synthesis, characterization, magnetic properties, and lead sensing based on a new alluaudite-like phosphate $\text{Na}_2\text{Mn}_2\text{Cr}(\text{PO}_4)_3$. *J Mater Sci* 56: 2163-2175. <https://doi.org/10.1007/s10853-020-05371-2>
- Lu J, Yamada A. 2016. Ionic and electronic transport in alluaudite $\text{Na}_{2-2x}\text{Fe}_{2-x}(\text{SO}_4)_3$. *Chem Electro Chem* 3(6): 902-905. <https://doi.org/10.1002/celec.201500535>
- Dwibedi D, Ling CD, Araujo RB, Chakraborty S, Duraisamy S, et al. 2016. Ionothermal synthesis of high-voltage alluaudite $\text{Na}_{2-2x}\text{Fe}_{2-x}(\text{SO}_4)_3$ sodium insertion compound: structural, electronic, and magnetic insights. *ACS Appl Mater Interfaces* 8(11): 6982-6991. <https://doi.org/10.1021/acsami.5b11302>
- Medvedeva NI, Buzlukov AL, Skachkov AV, Savina AA, Morozov VA, et al. 2019. Mechanism of sodium-ion diffusion in alluaudite-type $\text{Na}_5\text{Sc}(\text{MoO}_4)_4$ from NMR experiment and ab initio calculations. *J Phys Chem C* 123(8): 4729-4738. <https://doi.org/10.1021/acs.jpcc.8b11654>
- Dwibedi D, Araujo RB, Chakraborty S, Shanbogh PP, Sundaram NG, et al. 2015. $\text{Na}_{2.44}\text{Mn}_{1.79}(\text{SO}_4)_3$: a new member of the alluaudite family of insertion compounds for sodium ion batteries. *J Mater Chem A* 3(36): 18564-18571. <https://doi.org/10.1039/c5ta04527d>
- Liu D, Palmore GTR. 2017. Synthesis, crystal structure, and electrochemical properties of alluaudite $\text{Na}_{1.702}\text{Fe}_3(\text{PO}_4)_3$ as a sodium-ion battery cathode. *ACS Sustain Chem Eng* 5(7): 5766-5771. <https://doi.org/10.1021/acssuschemeng.7b00371>
- Dwibedi D, Jaschin PW, Gond R, Barpanda P. 2018. Revisiting the alluaudite $\text{NaMnFe}_2(\text{PO}_4)_3$ sodium insertion material: structural, diffusional and electrochemical insights. *Electrochim Acta* 283: 850-857. <https://doi.org/10.1016/j.electacta.2018.06.178>
- Plewa A, Kulka A, Baster D, Molenda J. 2019. An alluaudite compounds $\text{Na}_3\text{Fe}_2(\text{SO}_4)_3$ vs. $\text{Na}_{2.5}\text{Fe}_{1.75}(\text{SO}_4)_3$ as earth abundant cathode materials for Na-ion batteries. *Solid State Ionics* 335: 15-22. <https://doi.org/10.1016/j.ssi.2019.02.007>
- Hadouchi M, Assani A, Saadi M, Saadouni I, Lahmar A, et al. 2018. Synthesis, crystal structure and properties of a new phosphate, $\text{Na}_2\text{Co}_2\text{Cr}(\text{PO}_4)_3$. *J Inorg Organomet Polym Mater* 28: 2854-2864. <https://doi.org/10.1007/s10904-018-0956-y>
- Hadouchi M, Assani A, Saadi M, El Ammari L. 2016. The alluaudite-type crystal structures of $\text{Na}_2(\text{Fe}/\text{Co})_2\text{Co}(\text{VO}_4)_3$ and $\text{Ag}_2(\text{Fe}/\text{Co})_2\text{Co}(\text{VO}_4)_3$. *Acta Cryst Sec E Cryst Commun* 72(7): 1017-1020. <https://doi.org/10.1107/S2056989016009981>
- Bruker SAINT-Plus. 2012. Bruker AXS Inc., Madison, Wisconsin, USA.
- Krause L, Herbst-Irmer R, Sheldrick GM, Stalke D. 2015. Comparison of silver and molybdenum microfocus X-ray sources for single-crystal structure determination. *J Appl Cryst* 48(1): 3-10. <https://doi.org/10.1107/S1600576714022985>
- Sheldrick GM. 2015. SHELXT-Integrated space-group and crystal-structure determination. *Acta Cryst Sec A Found Adv* 71(1): 3-8. <https://doi.org/10.1107/S2053273314026370>
- Sheldrick GM. 2015. Crystal structure refinement with SHELXL. *Acta Cryst Sec C Struct Chem* 71(1): 3-8. <https://doi.org/10.1107/S2053229614024218>
- Farrugia LJ. 2012. WinGX and ORTEP for Windows: an update. *J Appl Cryst* 45(4): 849-854. <https://doi.org/10.1107/S0021889812029111>
- Hidouri M, Lajmi B, Wattiaux A, Fournes L, Darriet J, et al. 2008. Structural investigation of the alluaudite-like mixed-valence iron phosphate: $\text{Na}_{1.25}\text{Mg}_{1.10}\text{Fe}_{1.90}(\text{PO}_4)_3$. *J Alloys Compd* 450(1-2): 301-305. <https://doi.org/10.1016/j.jallcom.2006.10.119>
- Khmiyas J, Assani A, Saadi M, El Ammari L. 2015. Crystal structure of a sodium, zinc and iron(III)-based non-stoichiometric phosphate with an alluaudite-like structure: $\text{Na}_{1.67}\text{Zn}_{1.67}\text{Fe}_{1.33}(\text{PO}_4)_3$. *Acta Cryst Sec E Cryst Commun* 71(6): 690-692. <https://doi.org/10.1107/S2056989015009767>